An experimental study on the application of radionuclide imaging in repair of the bone defect

Weimin Zhu[1], Daping Wang[1]*, Xiaojun Zhang[2], Wei Lu[1], Jianquan Liu[1], Liangquan Peng[1], Hao Li[1], Yun Han[1], Yanjun Zeng[2]*

[1] Department of Sports Medicine, Shenzhen Second People's Hospital, No.3002, Sungang W. Road, Futian district, Shenzhen, 518035, P.R. China. [2] Beijing University of Technology, 100 Pinglyuan, Chaoyang District, Beijing, 100124, P.R. China

Abstract

The aim of our study was to validate the effect of radionuclide imaging in early monitoring of the bone's reconstruction, the animal model of bone defect was made on the rabbits repaired with HA artificial bone. The ability of bone defect repair was evaluated by using radionuclide bone imaging at 2, 4, 8 and 12 weeks postoperatively. The results indicate that the experimental group stimulated more bone formation than that of the control group. The differences of the bone reconstruction ability were statistically significant ($p<0.05$). The nano-HA artificial has good bone conduction, and it can be used for the treatment of bone defects. Radionuclide imaging may be an effective and first choice method for the early monitoring of the bone's reconstruction.

KEY WORDS: hydroxyapatite, nanometer, artificial bone, bone defect, radionuclide imaging

INTRODUCTION

Hydroxyaptite (HA, $Ca_{10}(PO4)_6(OH)_2$) shows poor artificial bone mechanics. Its brittleness and low fatigue strength in physiological environment limit its use for load-bearing repair or substitute [1]. As biomaterials and nanotechnology develop, researchers gradually switch their attention to nano-HA for bone reconstruction purposes. The radionuclide bone imaging is a major technique for observing bone blood supply and metabolism. Because the distribution of radionuclide agents indirectly reflects the blood supply, metabolism and regeneration of the bone, it sensitively reveals the diseased site and the bone activity at an early stage. Since the 1970s, the radionuclide bone imaging has been used to assess the metabolism of bone minerals. The current research explored the ability of novel nano-HA artificial bone in repairing the large segmental bone defect of the radius and dynamically monitored the bone regeneration using the radionuclide bone imaging in order to evaluate the value of the radionuclide bone imaging for monitoring the bone reconstruction as a clinical application reference.

* Corresponding authors:
Daping Wang,
Department of Sports Medicine, Shenzhen Second People's Hospital, No.3002, Sungang W. Road, Futian district, Shenzhen, 518035, P.R. China
Tel: +86 755 83791866; Fax: +86 755 83356952;
e-mail: szhzwm@126.com

Yanjun Zeng,
Beijing University of Technology, 100 Pinglyuan, Chaoyang District, Beijing, 100124, P.R. China. Tel: +86 10 67391809
Fax: +86 10 67391809; e-mail: yjzeng@bjut.edu.cn

Submitted: 14 March 2011 / Accepted: 6 April 2011

MATERIALS AND METHODS

Material

Nano-HA

The novel nano-HA was developed in a joint effort by the Powder Metallurgy Research Center of Central South University and our hospital. The nano-HA powder was prepared using calcium nitrate and ammonium dihydrogen phosphate through the sol-gel synthesis method [2]. The average size of the power was less than 100nm. The Nano-HA artificial bone with evenly distributed pores was formulated using nano-HA powder on a wooden mode. The pore diameter was 100-300μm and the porosity was over 90% [3].

Radionuclide scanner

The single-photon emission computed tomography (SPECT) scanner was purchased from Pegasys Inc. (Tokyo, Japan). The radionuclide bone imaging procedure was conducted in partnership with the Department of Nuclear Medicine, Shenzhen Second People's Hospital (Shenzhen, China).

Preparation of radionuclide agent

The radionuclide agent, 99mTechnetium-methylenediphosphonate (99mTc-MDP), was purchased from Guangdong Xi'ai Nucleus Pharmaceutical Center (Guangzhou, China)

Animals

24 conventional male New Zealand white rabbits from a closed colony, ranging from 1.5-2.0kg were purchased from Southern Medical University's Center of Experimental Animals. The rabbits were randomized into the treatment

group (the bone defect was repaired with the nano-HA artificial bone) and the control group (the defect was repaired with the HA artificial bone) with 12 rabbits in each.

Methods

Establishment of the animal bone defect

Each animal was given an intravenous injection of 20 mg/kg ketamine hydrochloride through the ear vein. The left anterior limb was chosen for bone defect establishment [4]. The animal was locally denuded, sterilized and covered with pads at the operation site. A median incision was made on the radius to expose the radius trunk. The radius was sawed at 2.5cm from the proximal side, and at 15mm from the first incision [5, 6]. The fragment with periosteum between two incisions was removed. After the wound was flushed with normal saline, different artificial bones were implanted in animals from different groups, and the wound was sutured layer by layer. The operation limb was not fixated locally and the wound was not bound up. When animals were awake from anesthesia, they were returned to the cage and fed normally. 80 units of penicillin were injected intramuscularly each day for consecutively 3d post operation.

Radionuclide bone imaging

The rabbits were monitored through radionuclide bone imaging at 2, 4, 8, and 12 weeks post operation [7, 8]. Four animals were randomly selected at each time point and injected with ketamine hydrochloride through the ear vein. The infusion injector was left at the ear vein following anesthesia. The animals were fixated at the animal station and pushed to the SPECT center. Each animal was given an intravenous injection of 18.5 MBq/kg bolus 99mTc-MDP through the injector, and drug leakage was carefully observed. 20 images were collected at a speed of 1 image per second as the whole-body arterial blood images, i.g the blood-flow phase. 5 images at a speed of 5 images per minute were collected and the one in the middle was selected for comparison. 4h later, images at a speed of 1 image per 5 minutes were collected as the whole-body static images, i.g the static phase.

Image analysis and treatment

The Pegasys Software Package and the image method were applied to identify regions of interest (ROI) (0.5x1.0cm) at the intact side and the fractured side. The average counts from ROI at both sides and the intake ratio (average counts at the fractured side/average counts at the intact side) in two groups were recorded.

Statistical analysis

SPSS11.0 was applied to analyze the average counts and the intake ratio between two groups.

RESULTS

General condition

All rabbits revealed normal eating behaviors and activities post operation. No death or infections occurred postoperatively. At 1 week post operation, the wound healed by first intention, and the stitches wore off automatically. The animals showed unlimited normal walking activities.

Radionuclide bone imaging results

Blood-flow phase

There was no significant difference in the blood-flow phase between the treatment group and the control group at different time points. Following injection of radionuclide agents into the vein, the blood-flow images of systematic and local blood circulation were observed instantly, and the contour of organs was then revealed. There was little accumulation in bones with low radioactivity at both the fractured side and the intact side (Figure 1 and 2).

FIGURE 1. Radionuclide bone imaging photo of experimental group (Blood-flow phas)

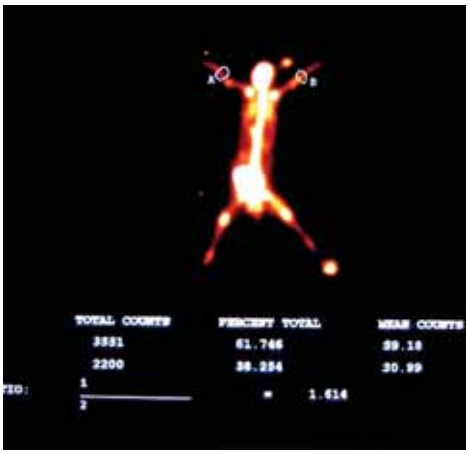

FIGURE 2. Radionuclide bone imaging photo and ROI Counting of control group (Blood-flow phas)

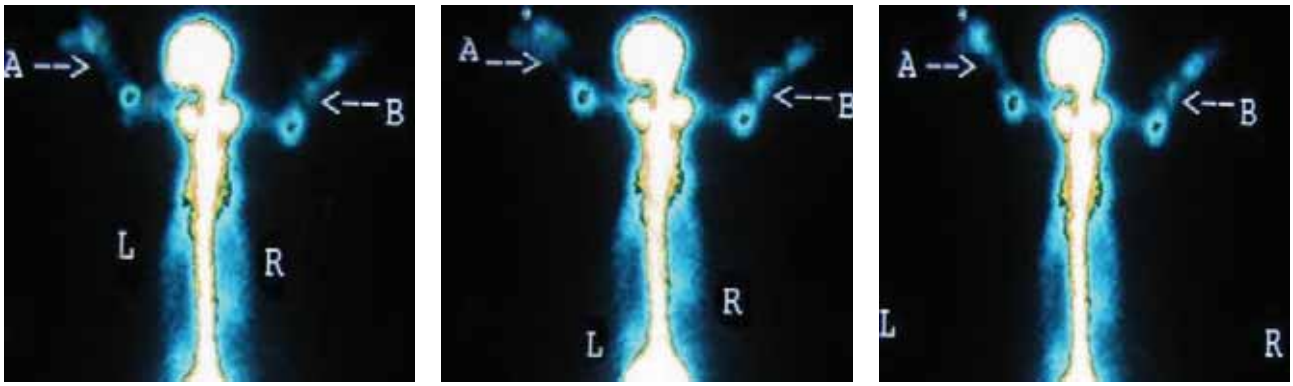

FIGURE 3-5. Radionuclide bone imaging photo of experimental group (4 weeks, 8 weeks, 12 weeks postoperatively, Blood-cistern phas, ROI counting level of operative limb increased progressively from 4 to 8 weeks postoperatively and descended 12 weeks postoperatively. ROI counting level of unaffected limb did not change).

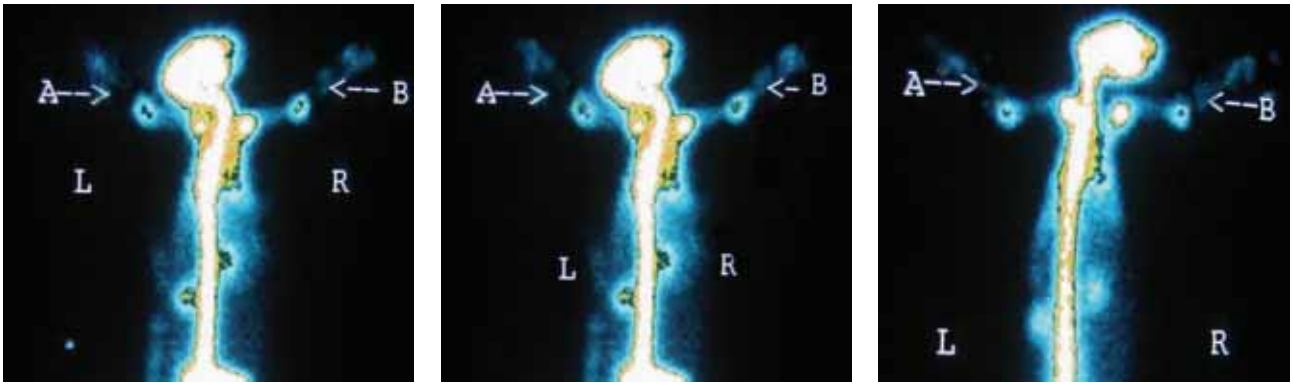

FIGURE 6-8. Radionuclide bone imaging photo of control group (4 weeks, 8 weeks, 12 weeks postoperatively, Blood-cistern phas, ROI counting level of operative limb increased progressively from 4 to 8 weeks postoperatively and descended 12 weeks postoperatively. ROI counting level of unaffected limb did not change).

Blood-pool phase

Radionuclide agents were mostly accumulated in blood-pool images. Soft tissues and organs over the body were clear with increased radioactivity that was distributed evenly images. The radioactivity in bones was low and the bones were not completely revealed (Figure 3-8). In blood-pool images, there was a statistically significant difference between the experiment group and the control group. The counts from ROI at the fractured side and the uptake ratio increased continually in the two groups at 2, 4 and 8 weeks, and started to decrease at 12 weeks. Statistical analysis showed that there were significant differences between 2 groups at different time points (p<0.05) and within 2 groups among different time points (P<0.05). The counts from ROI at the fractured side and the uptake ratio reached the peak at 8 weeks and decreased thereafter (Table 1 and 2).

TABLE 1. Counts from ROI in the blood-pool phase ($\overline{X}$ ±S, n=4)

Group	2 weeks	4 weeks	8 weeks	12 weeks
Treatment	2.91±0.45	6.90±0.88	10.18±0.96	7.22±0.66
Control	0.91±0.25	2.06±0.21	4.41±0.79	3.13±0.54

TABLE 2. Intake ratio in the blood-pool phase ($\overline{X}$ ±S, n=4)

Group	2 weeks	4 weeks	8 weeks	12 weeks
Treatment	2.39±0.30	5.90±0.94	10.51±0.95	7.13±0.96
Control	0.93±0.36	1.70±0.06	4.17±0.88	3.22±0.19

Static phase

In the static phase, radionuclide agents were mostly accumulated in bones in the treatment group and the control group. The bone joints, kidney, and bladder were clearly revealed with obvious radioactivity increase, indicating that most radionuclide agents are excreted through the urinary system. In the treatment group, the counts from ROI at the fractured side and the intake ratio increased continually at 2, 4 and 8 weeks, but started to decrease at 12 weeks at the fractured side. There was no apparent change in the counts from ROI at the fractured side and the intake ratio at the intact side as time went by. The counts from ROI at the fractured side were higher than the intact side at different time points. In the control group, the counts from ROI at the fractured side and the intake ratio increased before 8 weeks post operation at the fractured side, but not as obvious as in the experiment group. There was a statistically significant difference in the counts from ROI at the fractured side, and the intake ratio at 2, 4 and 8 weeks within the two groups (p <0.05). The counts

TABLE 3. Counts from ROI at the fractured side in the static phase ($\overline{X}$ ±S, n=4)

Group	2 weeks	4 weeks	8 weeks	12 weeks
Treatment	10.13±0.91	13.78±1.15	17.12±1.32	14.21±1.41
Control	5.90±1.14	7.85±1.00	12.19±0.92	8.70±1.26

TABLE 4. Intake ratio at the fractured side in the static phase ($\overline{X}$ ±S, n=4)

Group	2 weeks	4 weeks	8 weeks	12 weeks
Treatment	10.07±1.07	13.37±1.05	18.89±2.22	14.11±1.73
Control	6.39±1.33	8.36±0.67	11.49±1.47	8.86±1.07

from ROI at the fractured side and the intake ratio increased continually at the fractured side in the two groups as time went by. There was a statistically significant difference in the counts from ROI at the fractured side and the intake ratio at 8 and 12 weeks between two groups, and the counts from ROI at the fractured side and the intake ratio at 12 weeks decreased, compared to that at 8 weeks. There was a statistically significant difference between the two groups at different time points (2, 4, 8 and 12 weeks) (p<0.05) (Table 3-4), and the counts from ROI at the fractured side and the intake ratio at different time points were different between two groups (Figure 9-14).

DISCUSSION

Development of the HA artificial bone

Natural bones have a porous structure that bears forces within a range and maintains smooth blood flow ensuring normal growth and metabolism of bone tissues. As bone repair materials, the artificial bone should mimic the natural bone structure for bone regeneration. Mimicking, simulating and replicating the porous bone structure to develop bioactive and degradable porous bone repair materials remain a major research focus in biomaterial development. HA is highly bioactive and biocompatible that tends to well match the nature bone, and is a desirable supplement for bone defect. However, the HA ceramics has poor mechanical features that limit its use in areas of the bone that sustaining forces and thus is mainly applied in bone defect without force bearing. Researchers around the world have researched extensively to improve brittleness of HA. As the nanotechnology develops, researchers find that HA in the natural bone is mainly nanoscale needle-like monocrystals that align within the collagen matrix in a systematic manner. One study demonstrates that some materials due to "nanoscale phenomenon" may change in terms of mechanic

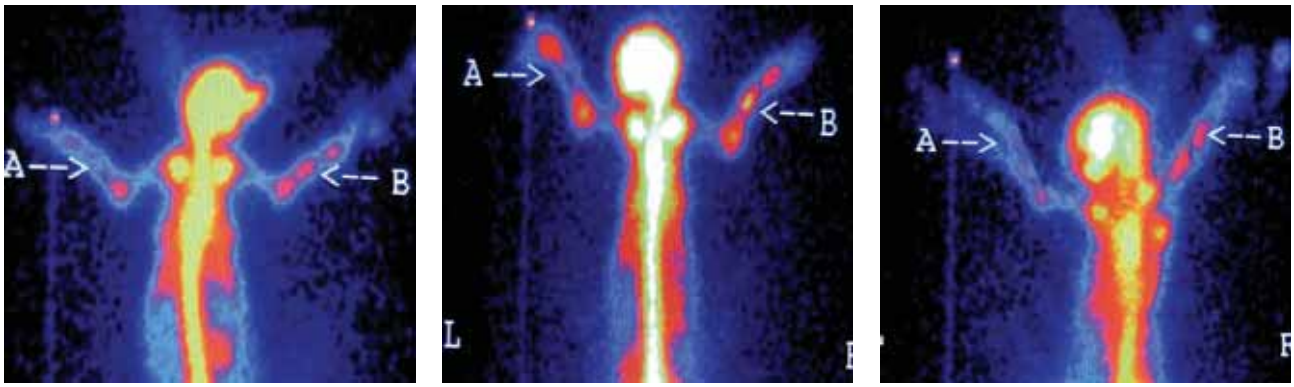

FIGURE 9-11. Radionuclide bone imaging photo of experimental group (4 weeks, 8 weeks, 12 weeks postoperatively, Static phase, ROI counting level of operative limb increased progressively from 4 to 8 weeks postoperatively and descended 12 weeks postoperatively. ROI counting level of unaffected limb did not change).

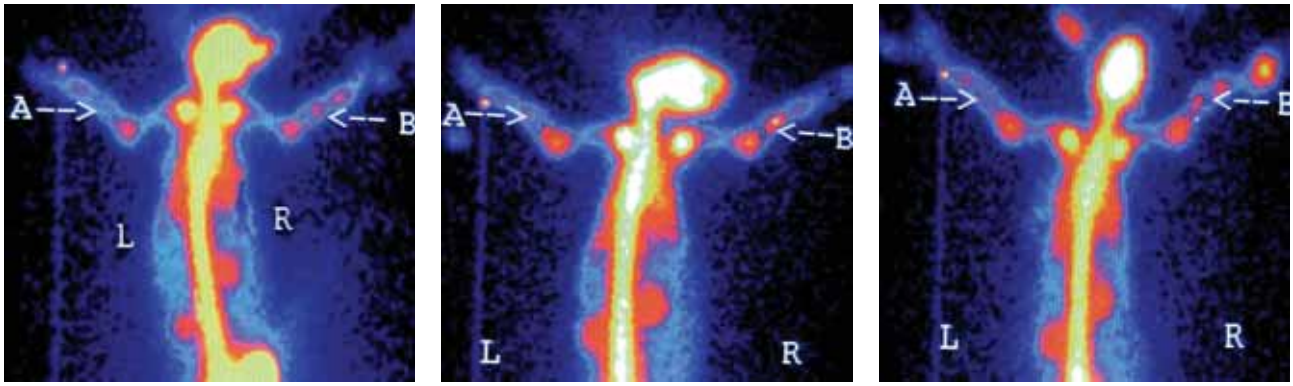

FIGURE 12-14. Radionuclide bone imaging photo of control group (4 weeks, 8 weeks, 12 weeks postoperatively, Static phase, ROI counting level of operative limb increased progressively from 4 to 8 weeks postoperatively and descended 12 weeks postoperatively. ROI counting level of unaffected limb did not change).

features when their particles are as small as the nanometer level [9]. When the particles are small enough, the torsion modulus, tensile modulus and tensile strength are high, and the fatigue resistance also increases. Nano-HPA are believed to have good biological and mechanical features [10]. Through years of research we develop the nano-HA artificial bone through the sol-gel synthesis approach using calcium nitrate and ammonium dihydrogen phosphate, and our testing data demonstrate the material has good biological features [11].

Radionuclide bone imaging in bone defect reconstruction

The rationale of radionuclide bone imaging is that, following venous injection or oral administration of radionuclide agents and composites, blood circulation, ion exchange and chemical absorption occur between them and positive/negative ions with different valence on the surface of HA, or they may combine to immature collagens that are revealed in imaging, as the bone contains minerals and collagens including HA [12, 13]. The two most important factors influencing the accumulation of radionuclide agents include (1) the integrity of blood supply and the rate of bone turnover [14]; (2) the bone metabolism, especially the bone regeneration rate; and (3) affinity of osteoid and immature collagen with 99mTc-MDP as well as alkaline phosphatase stimulation [15]. In recent years, as short half-life radionuclide agents are successfully developed and nuclear instruments and computer technology advance, the radionuclide imaging technique is enhanced and its application is thus expanded, rendering it as a major diagnostic technique for multiple bone and bone joint diseases especially in the early phase. Radionuclide agents accumulate when osteoblasts are active and new bones develop. Smelt et al. reported that the accuracy of prediction using radionuclide bone imaging reached nearly 100%. It has been shown that the radionuclide bone imaging is advantageous over X-ray in early diagnosis of femoral head necrosis, and reveals bone metabolism and bone formation at an early stage that ensures its use in monitoring early bone implant [16]. The current research explored radionuclide bone imaging in the blood-flow phase, the blood-pool phase and the static phase for reconstructed radius using the nanometer-HA in the rabbit. There is no statistically significant difference in the counts from ROI at the fractured side and the uptake ratio between the two groups at different time points in the blood-flow phase. An underlying cause is that the blood-flow phase mainly reflects perfusion in blood circulation and the large blood vessels on the bones. As there was no obvious damage to the local blood vessels, thus no significant difference is noted in the counts from ROI at the fractured side and the uptake ratio. The blood-pool phase mainly reflects the blood distribution in soft tissues over the body, while the static phase reveals the local bone metabolism. In the current research, there was 99mTc-MDP accumulation at the bone defect reconstruction site at 2 weeks, and increased gradually in both two groups, indicating that there is increased vascularization during bone reconstruction, the implant materials are bioactive, the local bone defect site undergoes obvious bone regeneration, and the bone metabolism increases. There is a statistically significant difference in the counts from ROI at the fracture side and the uptake ratio at different time points between two groups, showing that nano-HA and normal HA are significantly different in terms of bone reconstruction: the former is better than the latter in vascularization in the bone defect and bone regeneration that advances to be a promising bone repair material. In the current research, the radionuclide accumulation reached the peak at 8 weeks, and decreased thereafter, which is consistent with the timeline of bone repair and metabolism.

CONCLUSION

The results implies that the radionuclide bone imaging is valuable in revealing bone regeneration activity, and SPECT's monitoring function in bone repair promises a vision that the multiphase radionuclide imaging will be clinically used as a sensitive tool to monitor bone defect reconstruction.

ACKNOWLEDGMENTS

This study is given the pecuniary aid by the Guangdong Province science and technology planning project (the project number is 2010B031600028) and the Shenzhen science and technology planning project (the project number is 201002043).

DECLARATION OF INTEREST

The authors report no conflicts of interest. The authors alone are responsible for the content and writing of the paper.

REFERENCES

[1] Dorner-Reisel A, Klenn V, Irmer G, Muller E. Nano and microstructure of short fibre reinforced and unreinforced hydroxyaptite. Biomed Tech 2002; 47:397-400.
[2] Wan JM. China Patent: Produce Method of Polyporous Biomaterial. ZL 91106753.1 (2000. 1. 22).
[3] Zhu WM, Xiao JD, Wang DP. Experimental study of nano-HA artifi cial bone with different pore sizes for repairing the radial defect. Int Orthop, 2009; 2(33):1345-1350.
[4] Wang X, Li Y, Wei J, de Groot L. Development of biomimetic nanohydroxyapatite/poly(hexamethylene dipamide) composites. Biomaterials 2002; 23(24): 4787-4791
[5] Dorner-Reisel A, Klenn V, Irmer G, Muller E. Nano and microstructure of short fibre reinforced and unreinforced hydroxyaptite. Biomed Tech 2002; 47 suppl 1 Pt2:400-403.

[6] Zhou L, Zhao J, Shang H, Liu W, Feng Z, Liu G, Wang J, Liu Y. Reconstruction of mandibular defects using a custom-made titanium tray in combination with autologous cancellous bone. J Oral Maxillofac Surg. 2011, 69(5):1508-18.
[7] Nutton RW, Fitzgerald RH, Browm MI. Dynamic radiois otope bone imagine as a noninvasive indicator of canine tibial blood flow. Orthop Res 1984; 2(1):67-74.
[8] Genant HK. Bone seeking radionuclides:an in vitro study of factors affecting skeletal uptake. Radiology 1979; 113(6):373-375.
[9] Zhu W, Zhang X, Wang D. Experimental study on the conduction function of nano-hydroxyapatite artifi cial bone. Micro Nano Lett, 2010; 1(5):19-27.
[10] Holmberg S, Thorngren KG. Synthesis of biodegradable and biocompatible metrices with lysine diisocyantate and glycerol/glucose and other hydroxyl group donors Artaorthopscand Artaorthopscand 1984; 55(4):430-435.
[11] Sun MY, Ding HC, Mao TQ. RadionLClide Observation on Composite Grafts of Allogeneic Bone Matrix Gelatin and Partially Deproteinized Xemgeneic Bone. Orthop J Chin 2003;11(12):86-91
[12] Smeele LE, Heedstra OS, Wintes HA. Clinical effective of 99mTc diphosphonate scintigraphy of revascularized iliac crest flaps. Int J Oral Maxillofac Surg 1996;25:366-369.
[13] San SB, Dong SA, Jiang YM. Evaluation of 98mTc-MDP bone imaging in monitoring, the experimental bone allografts. Nuclear Techniques 1996; 19(5):31-34.
[14] Weimin Zhu, Daping Wang, Xiaojun Zhang, et al. Experimental Study of Nano-Hydroxyapatite/Recombinant Human Bone Morphogenetic Protein-2 Composite Artifi cial Bone. Artif Cell Blood Sub, 2010, 38: 150–156
[15] Nuzzo G, Luongo M, Parlato C, Moraci A. Cranial reconstruction using bioabsorbable calcified triglyceride bone cement. J Craniofac Surg. 2010; 21(4):1170-4.
[16] Iwakami T, Imai T. Effect of hydroxya patite sol on cell proliferation and alkaline phosphatase activity of osteoblastic MC3T3-E1 cells. Biomed Mater Eng 2002; 12(3): 249-257.